Silver, E. A., Rangin, C., von Breymann, M. T., et al., 1991
Proceedings of the Ocean Drilling Program, Scientific Results, Vol. 124

29. STABLE ISOTOPIC AND GEOCHEMICAL RECORD IN THE SULU SEA DURING THE LAST 750 K.Y.: ASSESSMENT OF SURFACE WATER VARIABILITY AND PALEOPRODUCTIVITY CHANGES[1]

Braddock K. Linsley[2,3] and Marta T. von Breymann[4]

ABSTRACT

Deep marine late Pleistocene sediments from Ocean Drilling Program Sulu Sea Site 769 contain a high-resolution record of paleoceanographic change in this strongly monsoonal climatic setting in the tropical western Pacific. Detailed time series of planktonic foraminifer (*G.ruber*; white variety) $\delta^{18}O$, $\delta^{13}C$, and bulk $CaCO_3$ mass accumulation rate (MAR) were generated, spanning the last 750 k.y. Sedimentation rates in this portion of the record average 8.5 cm/k.y., and vary from 4 to 16 cm/k.y.

Cross spectral analysis of the $\delta^{18}O$ and $\delta^{13}C$ time-series demonstrate that each contains increased variance at the primary orbital periodicities. The $\delta^{18}O$ record shows strong variability in the precessional-band and closely correlates with the SPECMAP $\delta^{18}O$ record and other high-resolution records. The dominance of a 23-k.y cycle in the $\delta^{18}O$ record agrees with other studies of the monsoon system in the Indian Ocean that have documented the importance of precessional insolation as a monsoon-forcing mechanism.

In addition, $\delta^{13}C$ is strongly coherent, with $\delta^{18}O$ at a period of 41 k.y (obliquity), suggesting a connection between surface water CO_2 chemistry in the Sulu Sea and high- latitude climatic change. The $\delta^{18}O$ and $\delta^{13}C$ time-series both contain increased spectral variance at a period of 30 k.y. Although the source of 30-k.y. variability is unknown, other studies have documented late Pleistocene Pacific oceanographic variability with a period of 30 k.y.

Major- and trace-metal analyses were performed on a second, less-detailed sample series to independently assess paleoproductivity changes and bottom-water conditions through time. Glacial periods are generally times of increased calcium carbonate and copper accumulation. The positive association between these independent indicators of paleoproductivity suggests an increase in productivity in the basin during most glacial episodes.

Changing bottom-water redox conditions were also assessed using the geochemical data. Low concentrations of molybdenum throughout the record demonstrate that bottom waters at this site were never anoxic during the last 750 k.y. The bioturbated character of the sediments agrees with this interpretation.

INTRODUCTION

Documenting Pleistocene climatic changes in the Indonesian tropics will be an important step toward understanding circum-Pacific climatic variability. The Sulu Sea in the humid Indonesian tropics of the western Pacific is a deep basin (>4800 m) completely surrounded by a shelf, most of which is less than 100 m deep (Figs. 1 and 2). High sedimentation rates and continuous deposition throughout the Pleistocene make deep marine sediments within the basin an excellent monitor of oceanographic change in the region.

The paleoceanographic record preserved in the Sulu Sea is important because surface-layer oceanographic conditions in the basin are directly controlled by the monsoonal climatic system of the Indonesian region and by the quasi-permanent Indonesian low-pressure system. This low-pressure system is important both because of its influence on the Indonesian monsoon and also for its role in the Southern Oscillation (SO). The Indonesian region has recently been noted for its large contribution to the interocean exchange of thermocline water (Gordon, 1986; Murray and Arief, 1988; Street-Perrott and Perrott, 1990). Large-scale exchange of upper ocean water from Indonesia to the Indian Ocean and into the Atlantic may influence the production of North Atlantic Deep Water (Street-Perrott and Perrott, 1990).

Tropical monsoonal climatic conditions and tectonic activity in the region have created one of the highest fluxes of river-borne sediment in the world (Milliman and Meade, 1983); consequently, sedimentation rates in the region are generally high. The isolated configuration of the Sulu Sea restricts circulation in the basin, resulting in anomalously warm and dysaerobic deep waters. The low dissolved oxygen content of intermediate and deep waters combined with high sediment accumulation rates has resulted in reduced benthic mixing of sediments. In addition, the anomalously warm deep waters (10°C) have led to enhanced carbonate preservation compared to the open western Pacific, also aiding in the preservation of high-resolution paleoclimatic records (Linsley et al., 1985).

The Indonesian region was climatically important during the Pleistocene because vast areas of shallow shelves were exposed during sea-level low-stands. The emergence of these shallow shelf areas during glacial stages may be responsible for Pleistocene variability of the Indonesian monsoon by changing the distribution of land and sea (Quinn, 1974; Bowler et al., 1976; Webster and Streten, 1978) and would also have influenced the exchange of thermocline waters with the Indian Ocean (COHMAP, 1988). Sea-level changes would also have strongly influenced oceanographic conditions in the Sulu Sea, where a conservative sea-level drop of 120 m during the last glacial maximum (Curray, 1964; Milliman and Emory, 1968; Fairbanks, 1989) is sufficient to almost totally isolate the basin from the surrounding seas, potentially changing surface and deep-water conditions.

[1] Silver, E. A., Rangin, C., von Breymann, M. T., et al., 1991. *Proc. ODP, Sci. Results*, 124: College Station, TX (Ocean Drilling Program).
[2] Department of Geology, University of New Mexico, Albuquerque, N.M. 87131, U.S.A.
[3] Present affiliation: Department of Geology and Geophysics, Rice University, Houston, TX 77251.
[4] Ocean Drilling Program, Texas A&M Research Park, 1000 Discovery Drive, College Station, TX 77845, U.S.A.

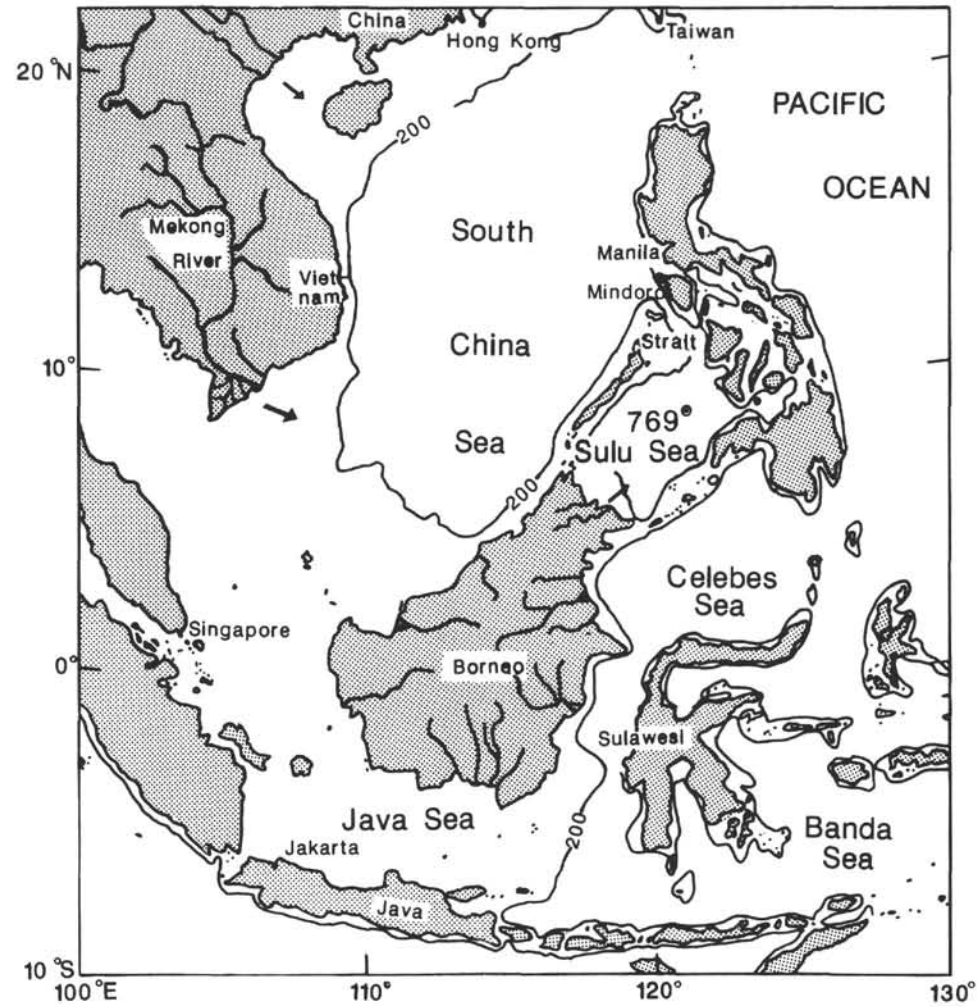

Figure 1. Map of western tropical Pacific showing location of the Sulu Sea and ODP Site 769. Bathymetric contour is the 200 m isobath.

Objectives, Sulu Sea Site 769

In this study, sediments from Site 769 spanning the last 750 k.y. were analyzed. This site is located in the Sulu Sea on the eastern flank of the Cagayan Ridge at 3644 m water depth on a bathymetric high well above the carbonate compensation depth (CCD), which is presently at 4800 m (Linsley et al., 1985) (Fig. 2). The location of Site 769 was chosen specifically to avoid turbidite sedimentation and to obtain a continuous, high-resolution Neogene paleoceanographic record. Preliminary shipboard results suggested that sediments deposited at Site 769 had high accumulation rates and potentially preserved a high-resolution record of oceanographic change in the basin.

Another objective of drilling in the Sulu Sea during Leg 124 was to determine the history of sediment redox conditions and history of bottom-water oxygenation in this restricted ocean basin. Based on organic carbon analyses and the oxygen and carbon isotopic composition of planktonic and benthic foraminifers, Linsley et al., (1985) had previously developed a paleocirculation model that shows an oxygen minimum expansion in the Sulu Sea during the last glacial maximum. They predict an increase in organic carbon preservation at mid-water depths throughout the basin at 18 k.y. B.P.

Holes 769A and 769B were hydraulically piston cored with overlapping sections to insure a complete late Pleistocene record. Whole-core paleomagnetic susceptibility results between Holes 769A and 769B show excellent correlation in the late Pleistocene portions of the record (Rangin, Silver, and von Breymann, et al., 1990). The similarity of magnetic susceptibility between these holes attests to the continuity of the sediment record at Site 769. The upper 65 m that was sampled for this study consists of a mixture of pelagic biogenic nannofossil marl with foraminifers and hemipelagic clay. The unit also has minor thin beds of volcanic ash and several foraminifer ooze turbidites. Time series of planktonic foraminifer $\delta^{18}O$, $\delta^{13}C$, total $CaCO_3$ mass accumulation rates (MAR), and major- and trace-element concentration data were generated for the last 750 k.y. of sediment record.

To evaluate water-mass conditions and primary productivity changes in the Sulu Sea during the last 750 k.y., an attempt was made to use the distributions of chemical components that might give independent information on paleoproductivity and paleoredox conditions in the Sulu Sea. This preliminary report describes these proxy records of surface-ocean and deep-water geochemical variability recorded at Site 769 and briefly discusses the possible climatic significance of late Pleistocene oceanographic variability in the western tropical Pacific.

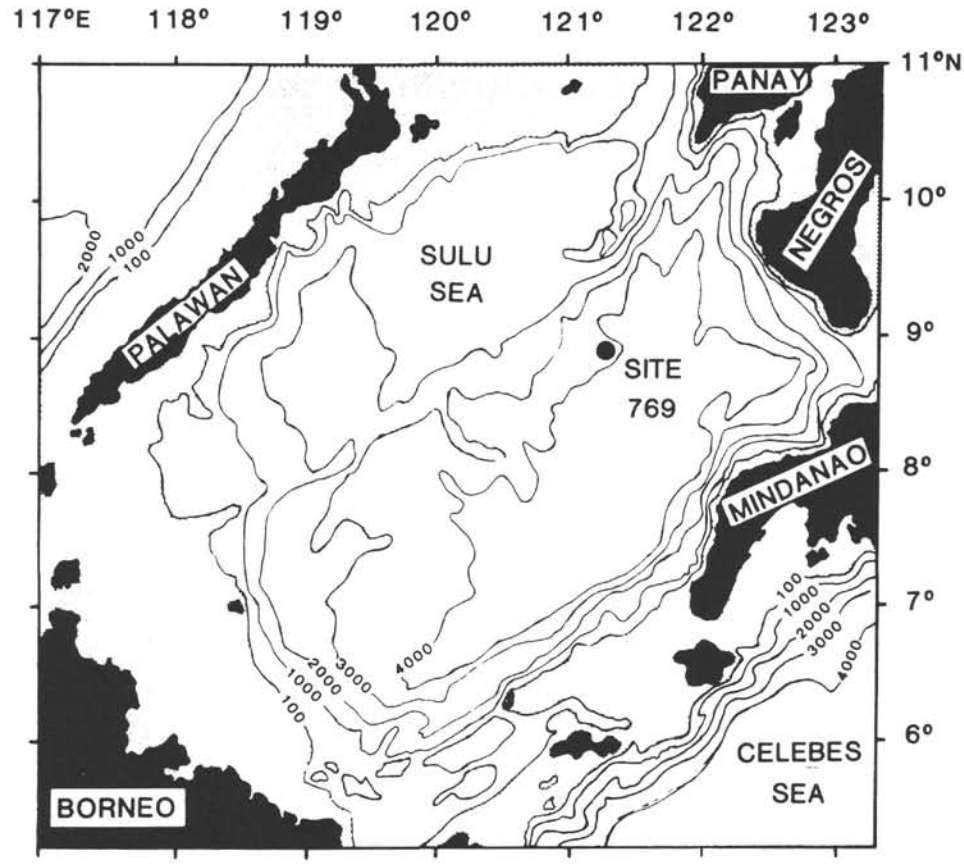

Figure 2. Detailed bathymetric map of the Sulu Sea (depths in meters). Shaded zone is that portion of the shelf shallower than 100 m. Note location of Hole 769 (3643-m water depth).

Regional Setting

The Sulu Sea is approximately 600 km long and 400 km wide, located between northern Borneo (Sabah) to the west and the central Philippine Archipelago to the east. A distinct northeast-trending bathymetric high, the Cagayan Ridge, subdivides the Sulu Sea into two sub-basins, the northwest Sulu Basin and the southeast Sulu Basin. The northwest basin has water depths ranging from 1000 to 2000 m. The southeast Sulu Basin is much deeper, with maximum depths between 4500 m and 5500 m along the Sulu Trench located off the Zamboanga Peninsula of Mindanao and Negros Island.

Surface-Water Hydrography

Surface waters of Southeast Asian seas have high temperatures and low salinities typical of humid tropical regions. There is an open exchange of surface water between the Sulu Sea and surrounding seas over the shelf and through channels in the shelf. The large excess of rainfall over evaporation creates an average surface salinity of 34‰. Annual temperature variations in the region are less than 2°C. Unlike temperature, salinity is extremely variable. This variability is a result of high rainfall and river runoff, and the intricate geographical structure of the area (Wyrtki, 1961). Surface-water circulation in the western equatorial Pacific is driven by the annually reversing monsoon winds creating large volumetric changes in surface water flow.

High temperatures and low salinities create surface waters of relatively low density compared with open Pacific Ocean waters. The less dense surface-water layer forms a strong contrast to the colder water masses at depth. The boundary between deep and surface waters occurs between 100 and 300 m and takes the form of a strong discontinuity layer permitting little vertical exchange of water. A thorough review of the surface-water hydrography of the Indonesian region is given by Wyrtki (1961).

Deep Water Hydrography

A shallow shelf, most of which is less than 100 m deep, completely surrounds the Sulu Sea (Figs. 1 and 2). Deep-water exchange is limited by the depth of the deepest sill supplying water to the Sulu Sea from the surrounding basins. The Mindoro strait along the east coast of Panay connects the basin to the South China Sea and is the deepest channel (420 m) into the Sulu Sea (Figs. 1 and 2). China Sea Intermediate Water only enters the Sulu Sea through the Mindoro Strait, thus this channel controls the ventilation rate of the basin (Frische and Quadfasel, 1990; Wyrtki, 1961; and Van Riel, 1943). Currently, deep water below the thermocline is uniformly warm (10°C), dysaerobic, and has the same physical properties as the water entering from the China Sea. At 600 m depth, temperatures are 10.5°C and vary less than 0.1°C, whereas salinities are 34.5‰ and vary less than ±0.5‰. From 600 to 4800 m depth temperature and salinity do not vary more than ±0.5°C and ±0.5‰, respectively (Fig. 3).

The concentration of dissolved oxygen is low throughout the deep waters (<1.2 mL/L). This dissolved oxygen concentration corresponds to only 20% saturation at the prevailing salinity and temperature.

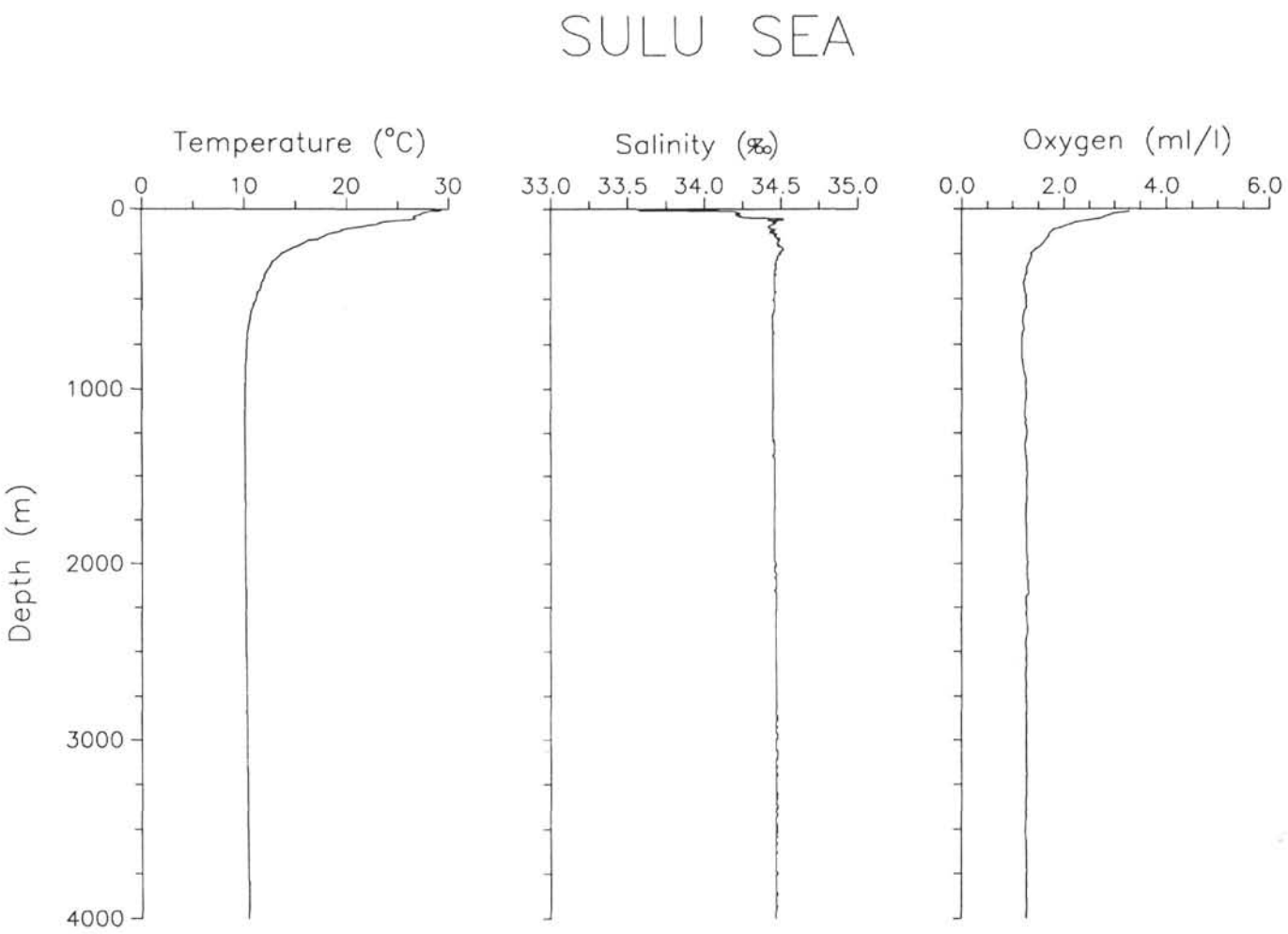

Figure 3. Temperature, salinity, and dissolved oxygen profiles from the Sulu Sea.

Warm bottom waters in the Sulu Sea result in excellent biogenic carbonate preservation. The CCD is currently at 4800 m while the carbonate lysocline occurs near 4000 m (Linsley et al., 1985; Exon et al., 1981; Thunell, unpubl. data). In contrast, the CCD and lysocline are at 4000 m and 3500 m, respectively, in the South China Sea, which is open to the western Pacific and is well-aerated at depth by cold bottom water (Rottman, 1979).

METHODS

The upper 65 m of sediment (last 750 k.y.) from ODP Hole 769A was sampled where possible at 20-cm intervals down through the Brunhes-Matuyama paleomagnetic reversal datum (730 k.y.), with the exception of the upper 4 m, which was sampled at 10-cm intervals. This sample series (n = 359) was analyzed for planktonic foraminifer $\delta^{18}O$ and $\delta^{13}C$, and bulk carbonate. Due to larger sample size requirements, major-element and trace metal concentrations were measured on a second sample series (n = 80) spanning the last 750 k.y. Excellent correlation of paleomagnetic susceptibility results between Holes 769A and 769B indicates no missing or overlapping sections (Rangin, Silver, von Breymann, et al., 1990, pp. 322–325).

Samples were freeze dried, and a split of each sample was analyzed for bulk $CaCO_3$. The carbonate content of the sediments was obtained by coulometric determination of the CO_2 liberated by HCL (2N) treatment of the sample, with replicate analyses yielding a standard deviation of ±0.5%. For planktonic foraminifer isotopic analysis the samples were wet sieved to remove the fraction < 63 μm. The planktonic foraminifer *Globigerinoides ruber* (white variety: 250–400-μm size) was used to construct $\delta^{18}O$ and $\delta^{13}C$ time series records for Hole 769A. Forty to fifty specimens were reacted at 50°C with 100% H_3PO_4, and the CO_2 gas was analyzed in a semi-automated VG Micromass 602E mass spectrometer at Rice University. Replicate analyses yielded a standard deviation from the mean of ± 0.09 ‰ for oxygen and ±0.08 ‰ for carbon. In 31 samples *G. ruber* was not in great enough abundance for isotopic work. In these cases *Neogloboquadrina dutertrei* was analyzed. In 10 samples comparing the *G. ruber* and *N. dutertrei* isotopic values, *N. dutertrei* had an average enrichment in ^{18}O of 1.09‰ (Std. Dev. = ± 0.21‰ and an enrichment in ^{13}C of 0.25‰ (Std. Dev. = ± 0.12‰). Based on these results the *N. dutertrei* isotopic compositions were corrected to the *G. ruber* data. Isotopic data are presented relative to the PDB standard in Table 1A (back-pocket microfiche). $CaCO_3$ data are listed in Table 1B.

Organic carbon (C-org) and trace-element concentrations were only determined for the smaller sample series. The organic carbon content was obtained by modification of the $H_3PO_4/K_2Cr_2O_7$ technique of Weliky et al. (1983), as described by Lyle et al. (1988). In this technique, inorganic calcium carbonate is first removed from a 300-mg sediment sample with phosphoric acid. The sample is then purged with

oxygen to remove any residual gas and treated with potassium dichromate for the determination of CO_2 by a Leco carbon analyzer with a thermal conductivity detector. This technique has been shown useful in working with samples with low organic carbon and high carbonate content.

The major and trace elements were determined by X-ray fluorescence (XRF) at the University of British Columbia, using a Phillips 1400 X-ray spectrometer. Major elements were analyzed using a fusion-heavy absorber method, while the samples for trace-element determination were prepared by pressing the samples with finely divided wax. Both techniques are described by Calvert (1990). The sediment geochemical data from this shorter sample series is presented in Table 2 (back-pocket microfiche).

Calculation of Mass Accumulation Rates

Bulk sediment and $CaCO_3$ mass accumulation rates (MAR), were calculated following the methods of Gardner et al., (1984). Due to the close sample spacing, the continuously measured wet-bulk density (WBD) obtained from the shipboard gamma-ray attenuation porosity evaluator (GRAPE) was used in the mass accumulation rate calculations. WBD was converted to dry-bulk density (DBD) by the following relationship (van Andel et al., 1975):

$$DBDg/cm^3 = WBDg/cm^3 - (0.01025 \times porosity) \quad (1)$$

The product of the average accumulation rates and the DBD gives bulk sediment MAR (g/cm²/k.y.). Mass accumulation rates of individual components were determined by multiplying the bulk accumulation rate by the weight fraction of the component in the sample.

ANALYTICAL RESULTS

Oxygen Isotopes and Age Model

The $\delta^{18}O$, $\delta^{13}C$, and calcium carbonate data have been plotted against time based on graphic correlation between this $\delta^{18}O$ data and the SPECMAP standard time scale (Imbrie et al., 1984), the position of the last appearance datum of *G. ruber* (pink variety) at 120 k.y. (Thompson et al., 1979) and the position of the Brunhes/Matuyama paleomagnetic reversal datum. The resulting time series of $\delta^{18}O$, $\delta^{13}C$, and $CaCO_3$ MAR are shown in Figures 4–6. Sedimentation rates in this portion of the record average 8.5 cm/k.y., and vary from 16 to 4 cm/k.y.

Calcium Carbonate Accumulation

The sediments collected at Site 769 are carbonate marls with $CaCO_3$ contents ranging from 11 to 55 wt.%. To assess the resolution of the MAR time-series, the $CaCO_3$ percentage data is shown in Figure 7 along with the bulk sediment accumulation rate. Low $CaCO_3$, and elevated bulk sediment accumulation occurs from 190–240 k.y. and from 460–625 k.y., suggesting terrigenous dilution of the carbonate record in these intervals. However, other variability in the carbonate record cannot be explained by sediment dilution and appears to be related to glacial/interglacial climatic changes. $CaCO_3$ accumulation generally increases during glacial times when global ice volume was expanded and sea level was lower. Exceptions occur at 120 k.y., 440 k.y., and 640 k.y., where high carbonate coincides with interglacials.

Time-Series Frequency Domain Results

To statistically evaluate the relationships between the $\delta^{18}O$, $\delta^{13}C$, and $CaCO_3$ MAR time-series seen in Figures 4–6, cross spectral analysis was performed. The cross spectra of $\delta^{18}O$-$\delta^{13}C$, $\delta^{18}O$-$CaCO_3$ MAR, and $\delta^{13}C$-$CaCO_3$ MAR time-series are displayed in Figures 8–10. Cross spectral results are discussed in terms of coherency and phase. Coherency is the linear correlation between two signals over a given frequency band when the phase difference is set to zero. If the spectral variance peaks of two time-series are aligned in a given frequency and the measure of coherency is greater than the 80% confidence level, then the linear relationship is judged to be statistically significant.

Phase differences have also been estimated between the three time series. These results are shown as phase angle vs. frequency plots in the lower half of Figures 8–10. The time-series were examined using standard time-series procedures (Jenkins and Watts, 1968). The data sets were first interpolated to equal time increments before generating the variance spectrums. One-third lags of the autovariance function were used to estimate the spectra. The average sample spacing of our data is 2500 yr corresponding to a maximum resolution (Nyquist period) of 5 k.y. Only those periodicities greater than 10 k.y. have been reported.

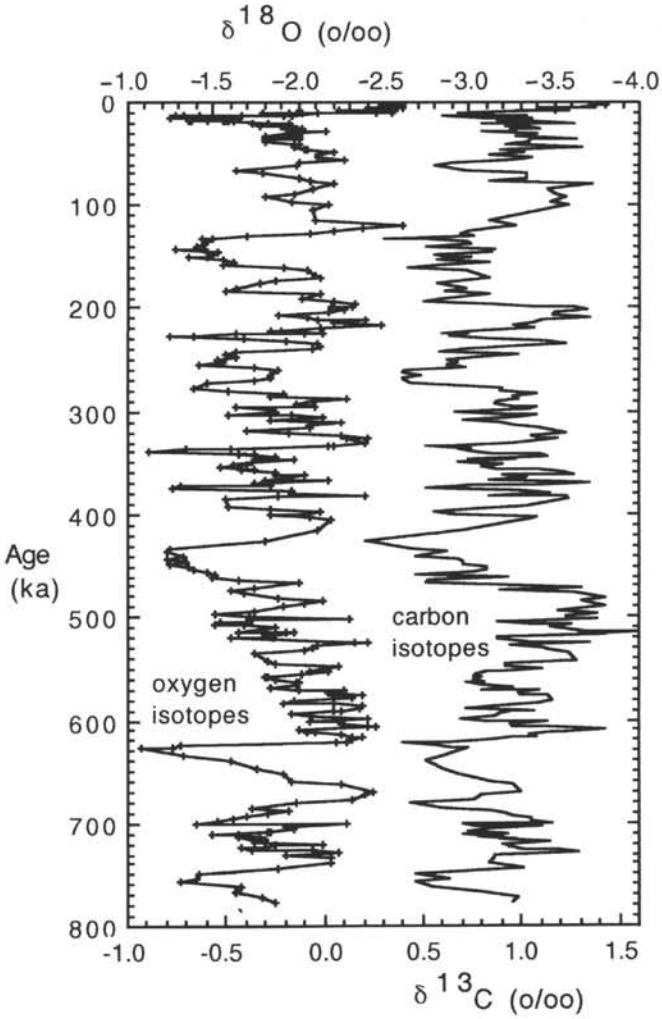

Figure 4. Time-series of $\delta^{18}O$ and $\delta^{13}C$ spanning the last 750,000 yr at Site 769A. Isotopic analyses are from *Globigerinoides ruber* (white variety). Age model derived from graphic correlation with SPECMAP stack (Imbrie et al., 1984), last appearance of *Globigerinoides ruber* (pink variety), and the position of the Brunhes/Matuyama paleomagnetic reversal datum.

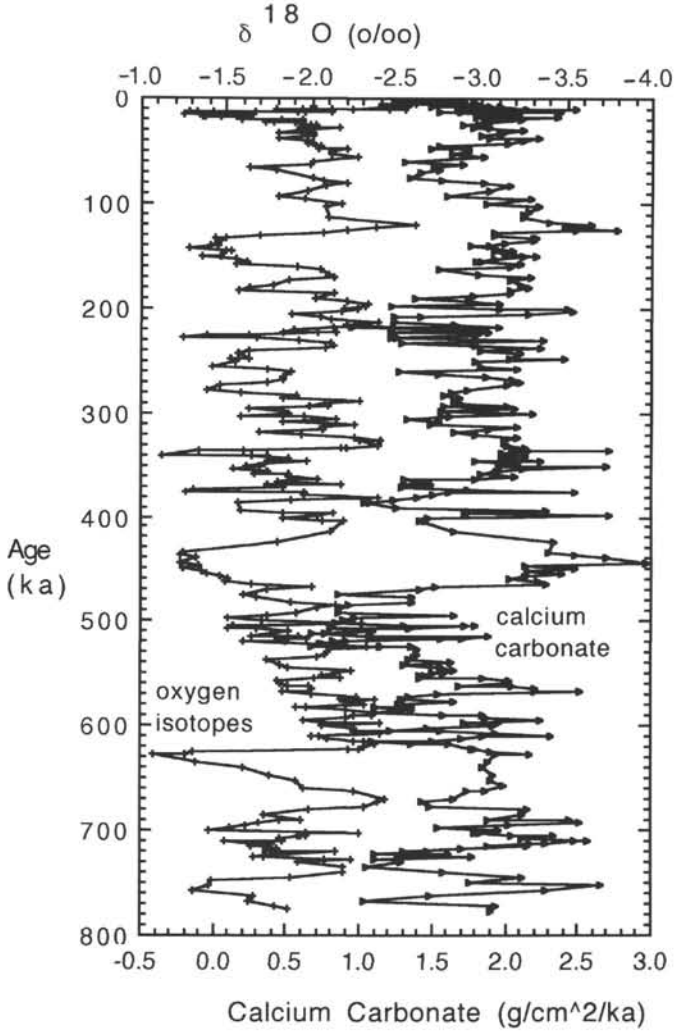

Figure 5. Site 769A; Time-series of $\delta^{18}O$ and $CaCO_3$ MAR ($g/cm^2/k.y.$).

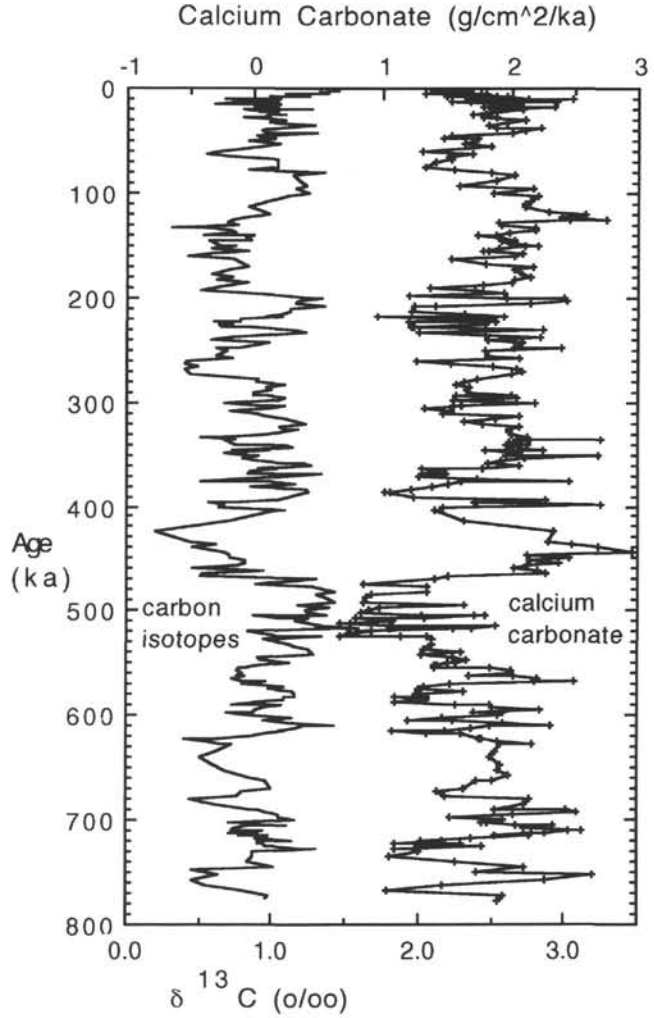

Figure 6. Site 769A; Time-series of $\delta^{13}C$ and $CaCO_3$ MAR ($g/cm^2/k.y.$).

The $\delta^{18}O$ record shows increased variance at the orbital periodicities of 100 k.y., 41 k.y., 23 k.y., and 19 k.y. (Figs. 8 and 9). In addition, a period of 30 k.y. occurs in this record of surface water $\delta^{18}O$ change. The planktonic $\delta^{13}C$ record also shows increased variance at periods of 100 k.y., 41 k.y., and 30 k.y., with a shift in the precessional band to a dominant period of 22 k.y. (Figs. 8 and 10). The calcium carbonate record contains eccentricity-band variability and a spectral peak near 28 k.y. (Figs. 9 and 10).

The $\delta^{18}O$ and $\delta^{13}C$ records are coherent at periods of 100 k.y., 41 k.y., and 30 k.y (80% level). Calcium carbonate accumulation is not coherent with $\delta^{13}C$, and is only coherent with $\delta^{18}O$ at a period of approximately 200 k.y. The phase angle plot indicates that $\delta^{18}O$ leads $\delta^{13}C$ in the 41-k.y and 30-k.y. frequency bands.

Organic Carbon, Major- and Trace-element Geochemistry

Discrimination of the chemical composition of the bulk sediment samples has been based on factor analysis. By factoring the data matrix of the components on a carbonate-free basis, the unrotated loadings of the first two factors explain a cumulative variance of 58%. The results are shown graphically in Figure 11. Factor 1 has high loadings for calcium carbonate, strontium, organic carbon, and copper. The organic carbon-carbonate covariance indicates a possible association with a productivity signal. The strontium fluctuations are due to the presence of coccoliths in these sediments (Rangin, Silver, von Breymann et al., 1990).

The $CaCO_3$, copper, and organic carbon data from this shorter sample series is displayed in Figure 12. Copper and $CaCO_3$ concentration trends generally follow each other. This relationship is strongest between 30 and 65 mbsf. The organic carbon content of these sediments is low, with values ranging from 0.02% to 0.41%. There is a large increase in organic carbon content in the upper 4 m of record, which was deposited during glacial stage 2.

Figure 13 displays the $\delta^{13}C$, copper, and calcium carbonate MAR data. The down core distributions show that times of high $CaCO_3$ accumulation generally coincide with high copper accumulation, and depleted $\delta^{13}C$ values in surface waters.

Factor 2 represents the nonbiogenic component. It shows that at this site, Fe, Cr, Al, Ti, and Ba enter the sediments in association with a detrital phase. Figure 14 shows that high levels of aluminum are coincident with periods of high sediment accumulation rates, clearly reflecting that the enhanced sedimentation rates result from increased loads of detrital

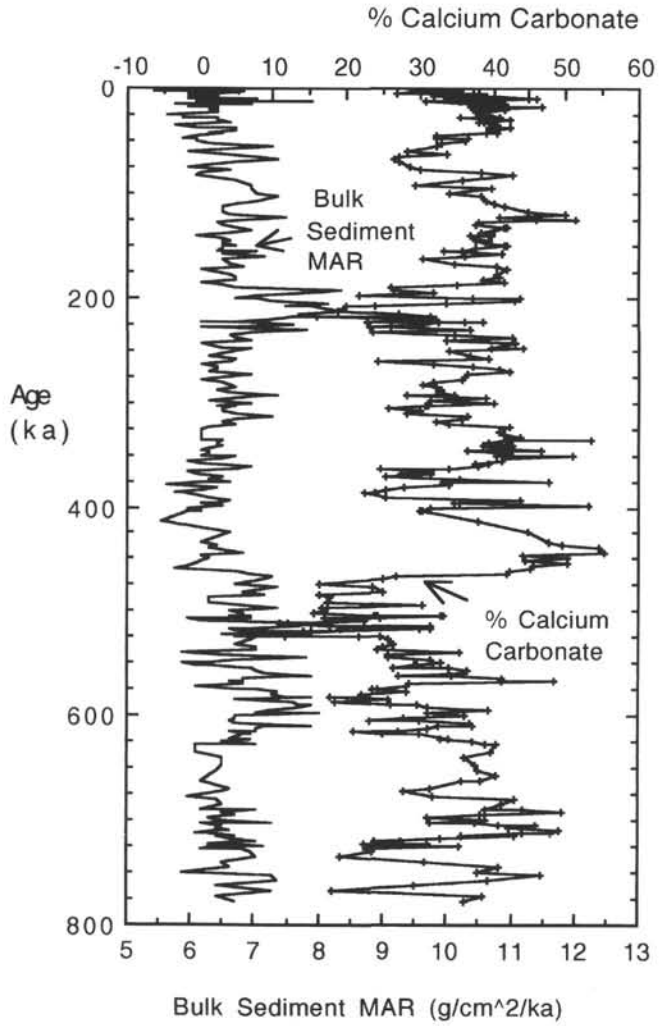

Figure 7. Time-series of bulk sediment accumulation rate (g/cm^2/k.y.), and % calcium carbonate. See Figure 5 for correspondence between glacials and carbonate accumulation.

components, either via atmospheric transport or increased river runoff. The high correlation of barium with aluminum is surprising because aluminum is considered to reflect the input of detrital aluminosilicates, whereas barium, in the form of barite, is thought to reflect biogenic input (Jumars et al., 1989; Bishop, 1988, Schmitz, 1987, and Dymond et al., unpubl. data).

DISCUSSION

Past Variability of Monsoon Systems

The importance of precessional insolation as a monsoon-forcing mechanism has been documented by numerous studies. In the Arabian Sea, Prell and Curry (1981) and Prell (1984a,b) through the use of planktonic foraminifer faunal records have demonstrated that the Indian monsoon has fluctuated in response to precessional changes in insolation. Global climate model (GCM) studies have verified the connection between increased monsoon winds and external insolation forcing over the axial precession cycle (Kutzbach, 1981: Kutzbach and Otto-Bliesner, 1982; Kutzbach and Guetter, 1986; COHMAP Members, 1988). Increased solar radiation results in a stronger monsoon circulation by increasing differential heating between southern Asia and the southern Indian Ocean. Other studies have shown that glacial periods in this monsoon region are more arid. Loess records from China (Kukla, 1987; Hovan et al., 1989; Kukla and An, 1989), lake-level studies from Africa, Arabia, and India (Street and Grove, 1979; Street-Perrott and Harrison, 1985), and the COHMAP (1988) study document increased aridity of glacial periods and humidity of interglacials in Arabia and central Asia. Similar changes were expected in the Indonesian monsoon system that controls oceanographic conditions in the Sulu Sea.

The Sulu Sea Site 769 Record

The Planktonic $\delta^{18}O$ and $\delta^{13}C$ Records

The oxygen and carbon isotopic records are based on *G. ruber,* which is a surface-dwelling planktonic foraminifer (Be and Tolderlund, 1971). Thus this species should be recording changes in surface water $\delta^{18}O$ and $\delta^{13}C$ chemistry. The magnitude of the $\delta^{18}O$ shift from maximum glacial to interglacial conditions is consistently 1.3‰, which is in agreement with previous results from this region (Linsley et al., 1985; Broecker et al., 1988; Quadfasel et al., 1990). The ice volume affect on the $\delta^{18}O$ record for the most recent glacial-interglacial transition is estimated to be 1.2‰, assuming that 10 m of sea-level rise is equivalent to a 0.11‰ change in $\delta^{18}O$ (Chappell and Shackleton, 1986; Labeyrie et al., 1987; Fairbanks, 1989). Thus, the overall glacial-interglacial $\delta^{18}O$ change in the Sulu Sea is primarily recording the global ice volume signal and not local surface-water temperature or salinity changes.

The late Pleistocene portion of the $\delta^{13}C$ record also appears to be consistent with other tropical $\delta^{13}C$ records. The $\delta^{13}C$ minimum that occurs at 10,000 yr B.P. is consistent with the deglacial $\delta^{13}C$ minimum found in many low-latitude planktonic records (Oppo and Fairbanks, 1989), suggesting that the $\delta^{13}C$ changes in Sulu Sea surface water are the result of a global low-latitude phenomenon.

Spectral analysis confirms the global nature of the $\delta^{18}O$ and $\delta^{13}C$ signals and the importance of precessional variability at Site 769 (Figs. 8–10). All the primary Milankovitch cycles are recorded with a strong component of precessional-band variability (Fig. 8), suggesting that the Indonesian monsoon has responded to precessional-band changes in solar radiation. Although the two time-series are not coherent in the precessional band they both contain increased variance in the 19- to 23- k.y frequency range.

The coherence of $\delta^{18}O$ and $\delta^{13}C$ at periods of 100 k.y., 41 k.y., and 30 k.y. also supports the conclusion that the $\delta^{13}C$ record has been forced by global-scale processes. The connection with the 41-k.y. obliquity cycle indicating a high-latitude forcing influence on the $\delta^{13}C$ record.

Several mechanisms could force the $\delta^{13}C$ variability in the Sulu Sea. The transfer of ^{13}C depleted carbon from forests and soils (Shackleton, 1977) to the tropical western Pacific could explain the observed decreases in planktonic $\delta^{13}C$ observed in the Sulu Sea record. This terrestrial influx could have led to the increased productivity suggested by the enriched copper and calcium carbonate concentrations (Fig. 11). Another way of explaining the low $\delta^{13}C$ values during glacial times is by the incorporation of "old" ^{13}C depleted deep water from below the surface mixed layer. This mechanism would require increased wind stress and a greater mixing depth in surface waters to account for the higher

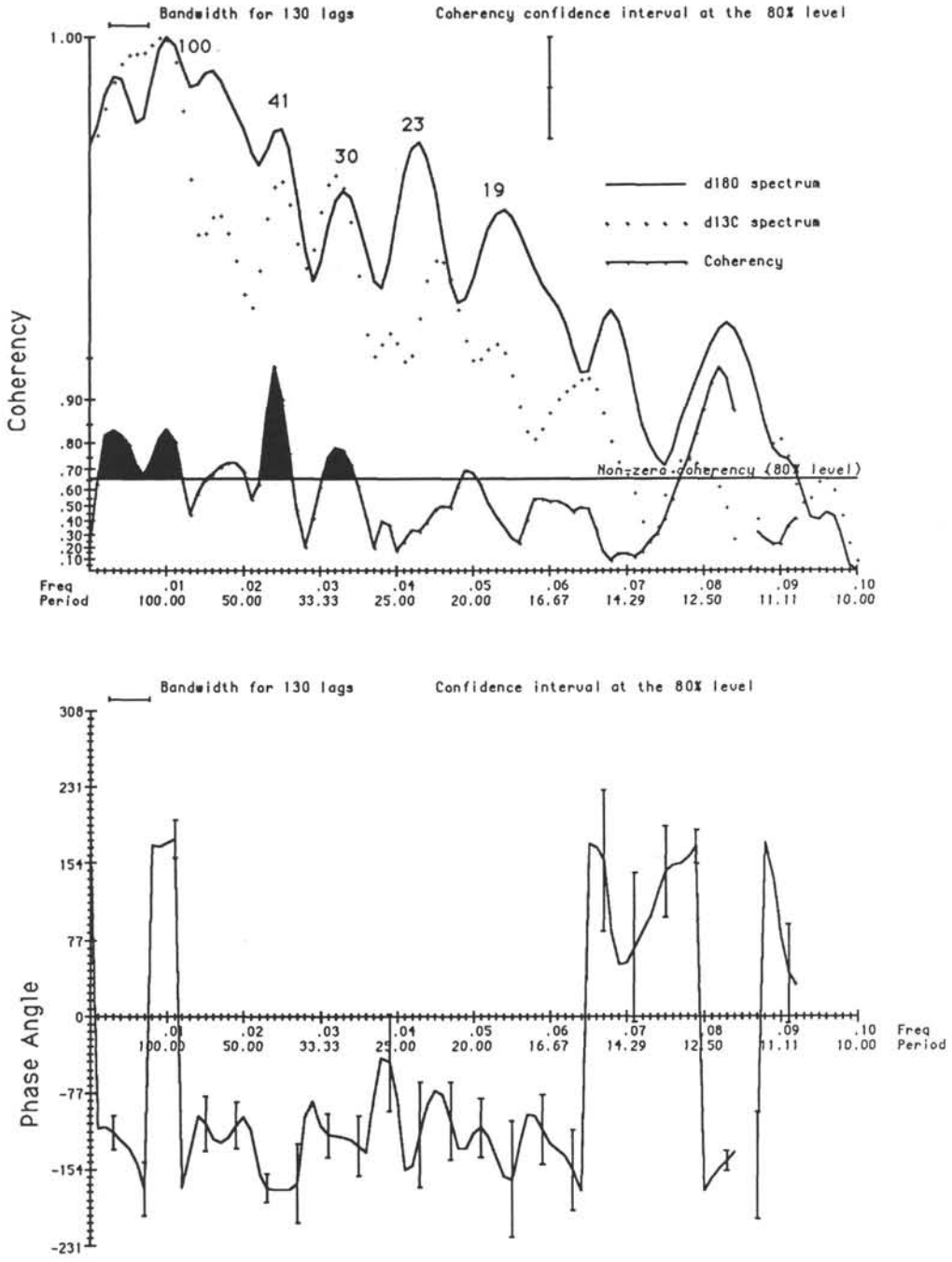

Figure 8. (Top) Spectral density and cross coherency for planktonic $\delta^{18}O$ and $\delta^{13}C$ at Site 769A (d18O and d13C, respectively). Spectral densities are normalized and plotted on log scales. The coherence spectrum (y-axis; solid line with pluses) is plotted on a hyperbolic arc-tangent scale. The solid horizontal line indicates confidence at the 80% level. Statistically significant coherence is indicated by shading. (Bottom) Phase angle vs. frequency plot. The y-axis is in degrees. To estimate lead or lag time at a given period, divide the phase angle by 360 and multiply by the period. Positive values indicate that the spectrum with the solid line leads the second series, and negative values indicate that this series lags the second series.

productivity during glacials. Presently we are not able to differentiate between which mechanism is responsible.

Although 30 k.y. is not a primary orbital period, Pisias and Rea (1988) found 30-k.y variability in late Pleistocene records in the central equatorial Pacific. They explained this period as a nonlinear response from the 100-k.y. and 41-k.y. cycles, which gives a period of 29 k.y. Beaufort and Aubrey (1990) have also found 30-k.y. variability in Pliocene calcareous nannofossil data from Site 552A in the North Atlantic. Clemens and Prell (1990) point out that a 35-k.y. cycle could result from the cross product of precession and obliquity. This evidence points to an inherent 30-k.y. cycle in the ocean-atmosphere system.

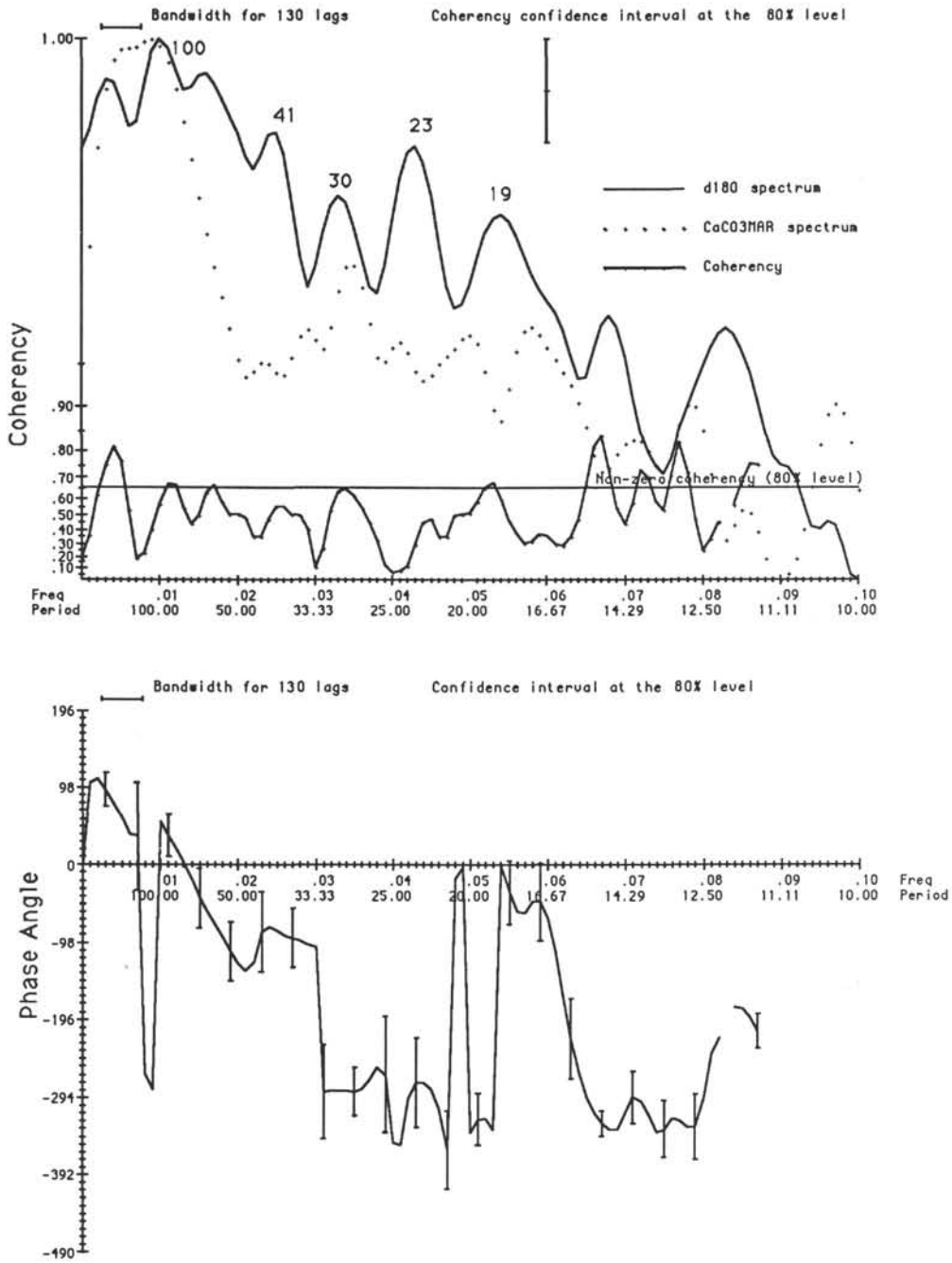

Figure 9. (Top) Spectral density and cross coherency for $\delta^{18}O$ and $CaCO_3$ MAR. (Bottom) Phase angle vs. frequency plot.

THE CARBONATE RECORD

Terrigenous Aluminosilicate Dilution of the Carbonate Record

Figure 14 shows that at the times of highest bulk accumulation rate (190–240, and 460–625 k.y.), the concentration of aluminum is also elevated. The abundance of $CaCO_3$ also decreases during these two times of higher bulk accumulation rates (Fig. 7). This evidence suggests that detrital dilution of the $CaCO_3$ MAR record occurred during these intervals. However, the majority of variability in the carbonate record cannot be explained by detrital sediment dilution and must result from carbonate preservation and/or carbonate productivity fluctuations.

Sill Depth and Carbonate Compensation Depth in the Sulu Sea

The shallowly silled configuration of the Sulu Sea and the dependence of its deep-water properties on sill depth make the basin a potential monitor of relative sea-level changes. An important question is how sea-level fluctuations during deglaciation affected the levels of the aragonite and carbonate compensation depths (ACD and CCD, respectively). A sea-level drop of 100 m is sufficient to almost completely isolate the Sulu Sea from surrounding basins. The deepest water

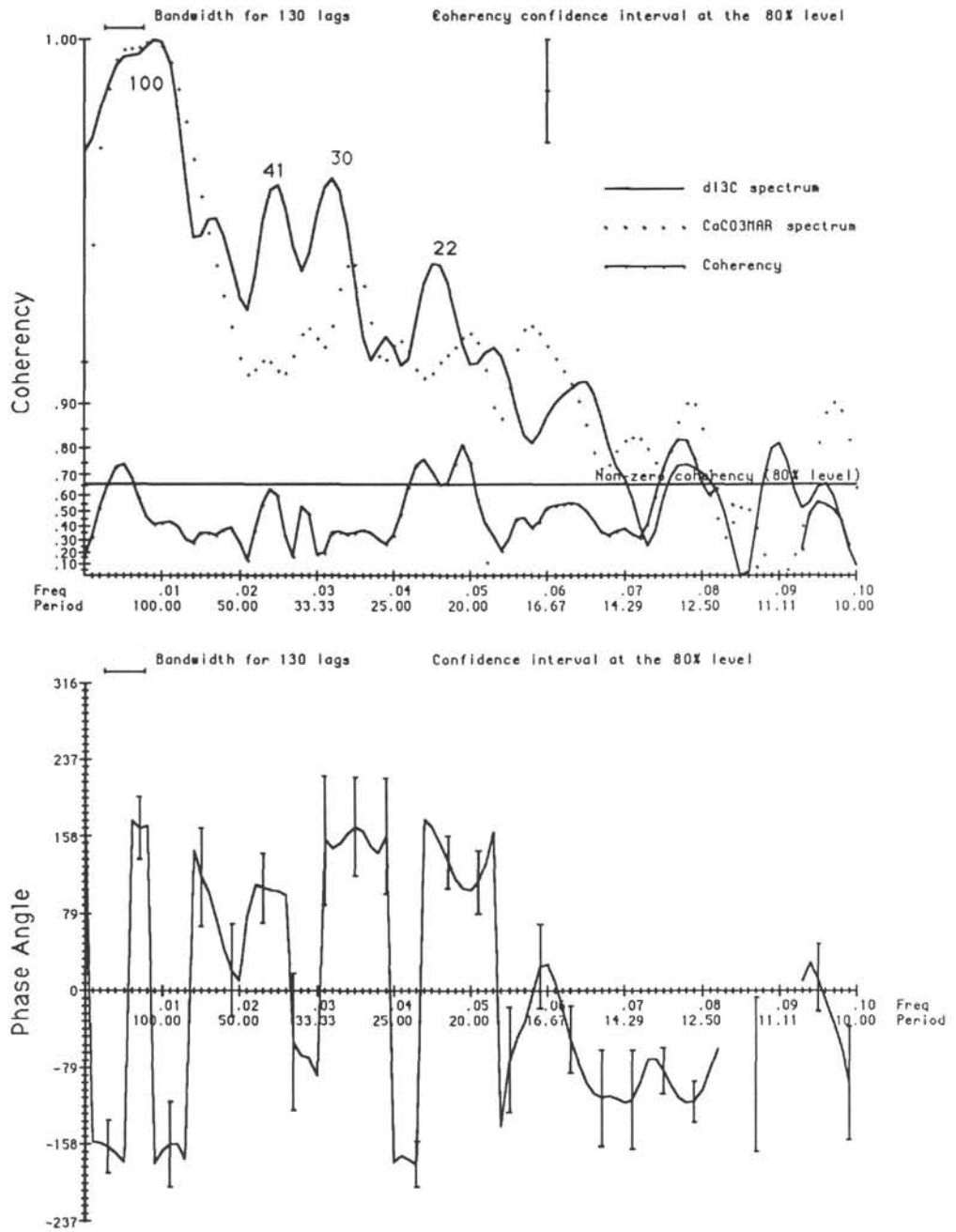

Figure 10. (Top) Spectral density and cross-coherency for $\delta^{13}C$ and $CaCO_3$ mass accumulation rates. (Bottom) Phase angle vs. frequency plot.

entering the basin would be originating higher in the water column compared to the present and could have been as much as 5°C warmer if the glacial thermal structure of the upper water column in the South China Sea was similar to that of today. The chemical composition of this water would also have been different than the densest water entering the Sulu Sea today. A shallowing of sill depth during glacial times could have caused a gradual warming of basin waters, coincident water chemistry changes, and potentially increased carbonate preservation.

The present-day aragonite compensation depth (ACD) in the Sulu Sea occurs at approximately 1400 m water depth (Linsley et al., 1985). However, pteropods were very abundant from 19 to 13 k.y. in Hole 769A (3640 m) (Linsley and Thunell, 1990), during the last glacial low-stand of sea level and in glacial stage 6 (128 to 186 k.y. B.P., Fig. 15). Piston cores RC14-78 at 1643 m and RC12-357 at 2049 in the basin also record large increases in the abundance of pteropods during this time, while two cores at water depths of 4102 m (V28-322) and 4480 m (V24-135) are devoid of pteropods during the last glacial maximum (see Linsley et al., 1985; Morgan, 1983). Thus, during the last glacial low-stand of sea level and glacial stage 6, when sea level was ~ 120 m below Holocene levels, the ACD in the Sulu Sea was 2200–2600 m deeper than the present level. Increased productivity and/or sea-level regulated bottom-water chemistry changes could have resulted in a lowering of the ACD level. The temperature affect on the saturation concentration of CO_3^{2-} is small com-

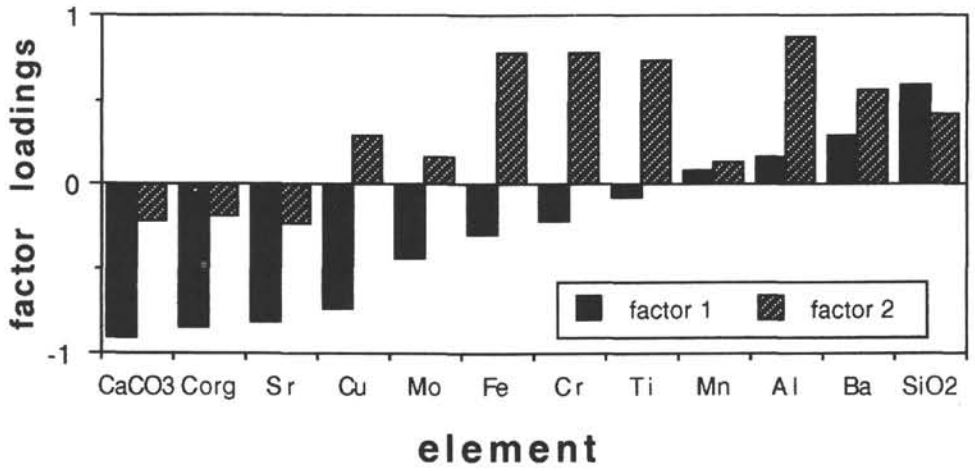

Figure 11. Factor loadings of the first two factors for the organic carbon, calcium carbonate, major- and trace-metal data. Note that calcium carbonate, strontium, and copper have high loading in Factor 1. Factor 2 (high aluminum, iron, titanium, chromium, and barium) represents the detrital component.

pared to the affects of carbonate primary productivity variations or variations in the carbonate ion content of sea water (Broecker and Peng, 1982). Thus, productivity or water chemistry changes are more likely responsible for deepening the ACD, than strictly bottom-water temperature changes.

Foraminifers are remarkably well preserved at Site 769A, with the exception of the intervals 390–408, 473–492, and 513–537 k.y. In these intervals bulk carbonate concentration is low and *G. ruber* and other dissolution susceptible planktonic foraminifer species are highly fragmented and partially dissolved. During these times it appears that the lysocline in the basin may have risen to 3600 m, the depth of Site 769. At no time in the past 750 k.y was the CCD as shallow as 3600 m.

Paleoproductivity

The factor analysis results indicate that at Site 769 there is a good correspondence between the organic carbon and the carbonate distributions during the last 750 k.y. However, Figure 12 shows that organic carbon content is very low in this record, with only minor variability. Using sediment-trap data, Lyle et al., (1988) have shown that when both opal-rich and carbonate-rich plankton communities contribute to the total biogenic flux, a better correlation with C-org is observed when both the opal and carbonate content are combined. Although there is evidence of a diatom contribution to the sediments at Site 769, there is intensive dissolution of this component. The diagenetic remobilization of opal was evident in the preservation of diatom tests as well as the dissolved silica profiles (Rangin, Silver, von Breymann et al., 1990). Therefore, no opal estimations were attempted in this study.

The problem of estimating paleoproduction from the sedimentary record is basically that most buried signals record bottom-arriving flux minus dissolution flux and not surface production directly, and that the bottom-arriving flux is also a function of the water column characteristics. Organic matter content, although itself a good paleoproductivity indicator, is strongly affected by degradation in the water column, at the sediment-water interface, and by sediment diagenesis. The distribution of organic matter is also affected by the amount of terrigenous components. These problems led investigators to pursue the use of other chemical parameters such as proxy-indicators of paleoproductivity. In the following section the distributions of barium and copper at Site 769 are discussed, two elements that have been shown to be promising as proxy-indicators for paleoproductivity.

Particulate fluxes of barium and organic carbon in sediment-trap samples have been used to establish a link between primary productivity and barium flux to the ocean floor (Dymond et al., unpubl. data). Furthermore, the barium distribution in marine sediments shows an enrichment underneath the equatorial divergence in the Pacific and Indian oceans (Fig. 16), and on this basis the barium concentration has been used as a paleoproductivity indicator (Jumars et al., 1988, Bishop, 1988, and Schmitz, 1987, Dymond et al., unpubl. data).

However, at Site 769 all the barium seems to be associated with the detrital component (Figs. 11 and 15). High barium levels are usually associated with high opal contents, which suggests that the mechanism that leads to barium enrichments, by active secretion from an organism, or by decomposition of planktonic organic matter, might be dependent on the presence of silica. A possible explanation for the lack of a barium component at this site might be that there is a depletion of this element in the water column. In addition, the Sulu Sea is apparently an area of low productivity. Although opal contents could not be measured due to its intensive diagenetic mobilization, a silica-depleted system might have resulted in the low barium levels measured at Site 769. The regeneration pattern of barium has been shown to result in maxima in the dissolved and particulate concentrations at a depth of several hundred meters (Bishop, 1988, and Dymond et al., unpubl. data). The presence of the shallow sill in this basin restricts the water flow from the South China Sea. This is reflected in the uniformly warm and dysaerobic water of the Sulu Sea below the thermocline (Frische and Quadfasel, 1990), and could have led to a barium-depleted system in the Sulu Basin.

Copper has been shown to correlate strongly with the biogenic component in sediment trap material (Fisher et al., 1986, Lyle and Collier, 1988), and to image areas of high productivity in the eastern equatorial Pacific (von Breymann et al., unpubl. data) and on the Oman margin (K. Emeis, pers comm., 1990). Copper is apparently removed from the water column by organic particles. Thus it has been recognized as a potential proxy indicator of organic matter accumulation (Lyle and Collier, 1988).

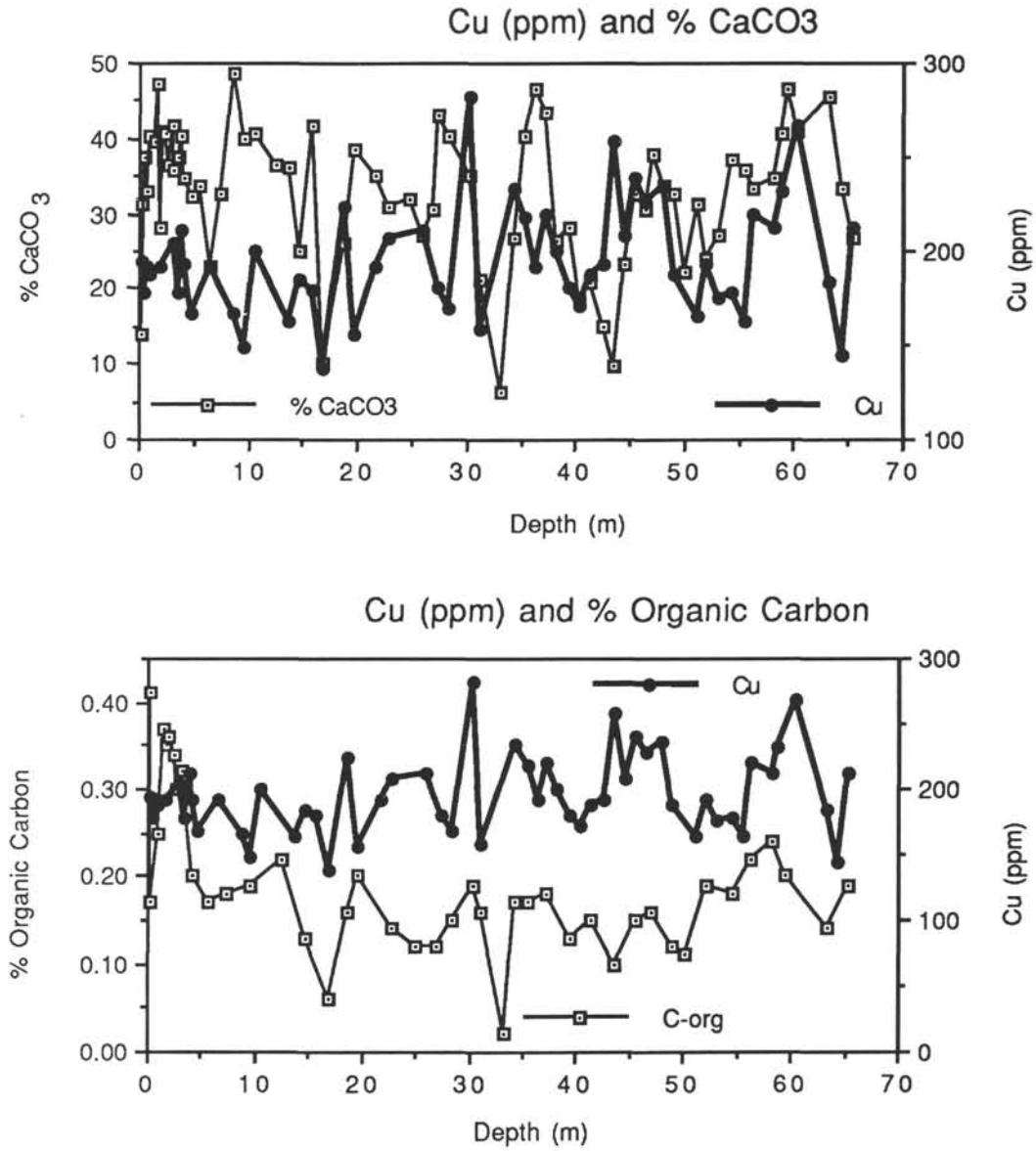

Figure 12. Down-hole distributions of $CaCO_3$, organic carbon, and copper at Site 769A.

Copper has significant loadings in factor 1 (Fig. 11), which suggests a nondetrital component in the copper distribution. This is also indicated in Figure 17, which shows an excess of copper relative to aluminum. The copper-organic carbon covariance suggests an increased flux of organic matter to the sediments during the periods of higher copper accumulation.

Copper and $CaCO_3$ measurements on the same samples both have significant loadings in Factor 1. This relationship is also seen in the plot of copper and $CaCO_3$ vs. age (Fig. 12). The copper-$CaCO_3$ relationship suggests that increased sedimentary $CaCO_3$ concentrations is the result of increased productivity. This is supported by the general correspondence of enhanced copper and CaCO3 MAR during glacial periods, suggesting that productivity increased during glacial times. However, it is not certain whether increased productivity results strictly from increased wind stress, river-borne nutrient flux, or from some combination of these factors.

Bottom-Water Paleo-Redox Conditions

Lowered sea level during glacial periods would further isolate the Sulu Sea from the surrounding basins and might have restricted deep-water ventilation in the basin. One objective of drilling in the Sulu Sea was to determine the history of sediment redox conditions and hence bottom-water dissolved oxygen levels. Did glacial isolation of the basin result in lowered dissolved oxygen levels in deep waters? Could an oxygen-depleted basin have resulted in periods of increased preservation of the organic carbon?

Molybdenum is enriched in marine sediments in association with the formation of manganese oxides, and in highly reducing conditions is associated with accumulation of organic matter and precipitation of sulfides. Typically, deep pelagic sediments contain 4 to 18 ppm of molybdenum. Enrichment of this element in sediments is a sensitive indicator of anoxic conditions, either via formation of molybdenum sulfides or by adsorption onto organic phases

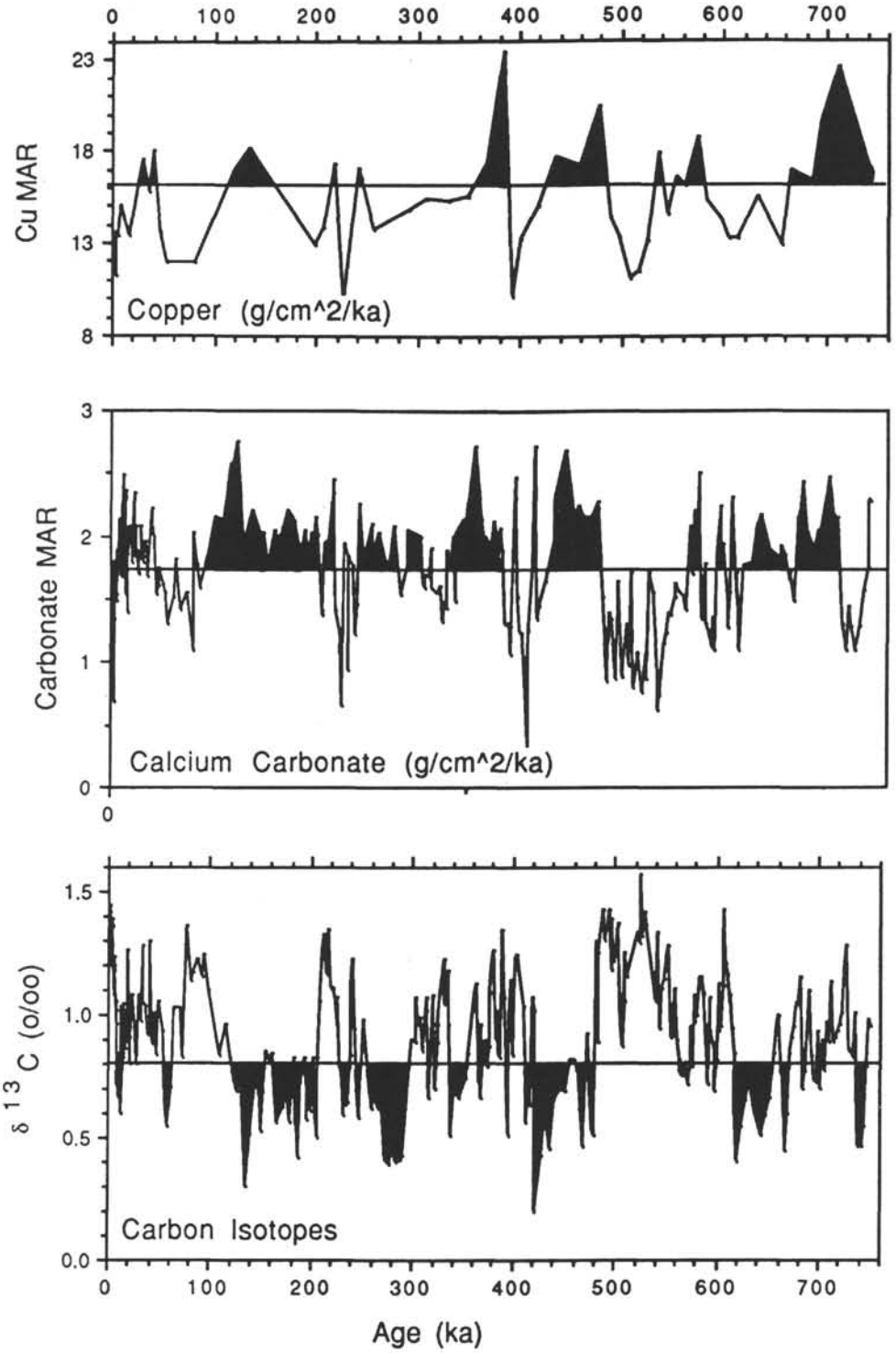

Figure 13. Time-series of Copper MAR, $CaCO_3$ MAR, and planktonic $\delta^{13}C$. Note that times of high copper accumulation generally correspond to times of high $CaCO_3$ accumulation and depleted $\delta^{13}C$.

(Bertine, 1972). High concentrations have been observed in continental margin upwelling zones, semi-enclosed bays and estuaries that are well supplied with nutrients and develop stratified water conditions, and landlocked seas of wide geographical extent, such as the Baltic and Black Seas (Calvert, 1976; Fig. 18). The Sulu Sea is dysaerobic today and the low levels of molybdenum observed at Site 769 negate the possibility of strongly anoxic conditions in this basin for the last 750 k.y.

There is, however, an approximate two-fold increase in the amount of organic matter preserved during the last glacial maximum at 18 k.y. relative to the rest of the record (Fig. 12). Such an increase is not observed in the carbonate or the copper records. An increased flux of terrestrial organic carbon

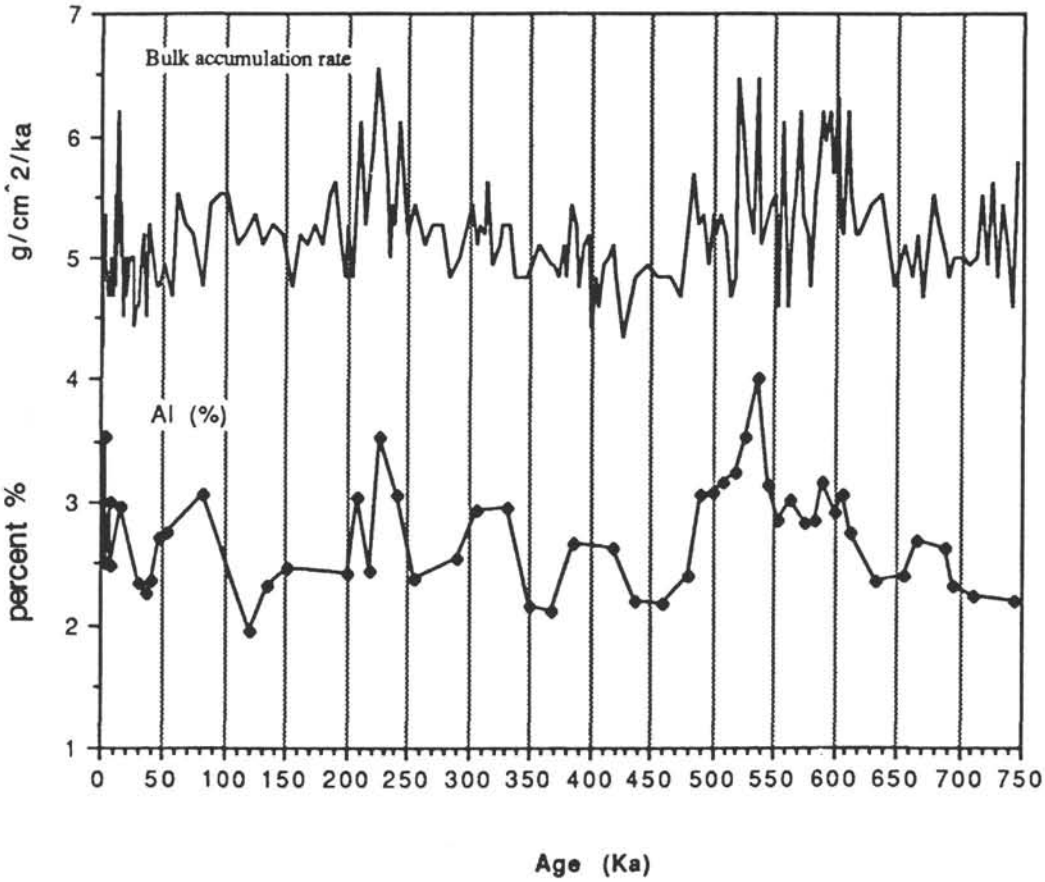

Figure 14. Time series of bulk sediment and aluminum accumulation at Site 769. High bulk accumulation rate generally coincides with elevated aluminum concentrations.

and/or increased preservation due to dysaerobic deep-water conditions may be responsible.

CONCLUSIONS

Late Pleistocene sediments from Site 769 in the Sulu Sea contain a continuous high-resolution record of paleoceanographic change in this climatically important region of the tropical western Pacific. Sedimentation rates in this portion of the record average 8.5 cm/k.y., and vary from 4 to 16 cm/k.y.

Detailed time-series of planktonic foraminifer (*G.ruber*; white variety) $\delta^{18}O$, $\delta^{13}C$, and bulk $CaCO_3$ mass accumulation rate (MAR) were generated, spanning the last 750 k.y. Spectral analysis indicates that both the $\delta^{18}O$ and $\delta^{13}C$ surface-water records contain increased spectral variance at periods of 100 k.y (eccentricity), 41 k.y (obliquity), 30 k.y., and 23 k.y (precession). The dominance of the precession cycle in forcing the $\delta^{13}C$ and $\delta^{18}O$ records indicates that changes in insolation over the Earth's axial precession cycle has influenced variability in the Indonesian monsoon system. The 30-k.y cyclicity in these time-series adds evidence supporting other results that have documented the presence of an inherent 30 k.y. climate cycle. The $\delta^{18}O$ and $\delta^{13}C$ records are coherent at periods of 100 k.y, 41 k.y, and 30 k.y. The strong obliquity-band variability in both records suggests a high-latitude effect on ^{13}C chemistry of surface waters in the tropical Pacific.

There is also a general correspondence between elevated copper and calcium carbonate concentration, and depleted planktonic $\delta^{13}C$ values during glacial periods in the Sulu Sea. Glacial low-stands of sea level are generally marked by increased accumulation of copper, and calcium carbonate. This correspondence between these independent indicators of paleoproductivity suggests an increase in productivity in the basin during glacial episodes.

Low concentrations of molybdenum throughout the record suggest that bottom waters at this site were never anoxic during the last 750 k.y.. However, high organic carbon contents during the last glacial period from 18 to 13 k.y., supports the earlier work of Linsley et al. (1985), who found evidence for low dissolved oxygen conditions at mid-water depths.

ACKNOWLEDGMENTS

We thank Robert Dunbar for use of the stable isotope facilities at Rice University, Steve Calvert for XRF analysis at the University of British Columbia, and Roger Y. Anderson for his comments. The paper has benefited from reviews by Nicklas Pisias, Walter Dean, and Graham Shimmield. In addition, we acknowledge the scientific members and crew of ODP leg 124 for their help. This research was supported by grants from the JOI U.S. Science Support Program to B. Linsley and M. von Breymann. The U.S. Science Program associated with the Ocean Drilling Program is sponsored by the National Science Foundation and the Joint Oceanographic Institutions, Inc.

REFERENCES

Bé, A.W.H., and Tolderlund, D. S., 1971. Distribution and ecology of living planktonic foraminifera in surface waters of the Atlantic and Pacific Oceans. *In* Funnel, B. M., and Riedel, W. R. (Eds.), *Micropaleontology of the Oceans:* Cambridge (Cambridge Univ. Press), 105–149.

Beaufort, L., Aubry, M.-P., 1990. Fluctuations in the composition of late Miocene calcareous nannofossil asemblages as a response to orbital forcing. *Paleoceanography,* 5:845–865.

Bertine, K. K., 1972. The deposition of molybdenium in anoxic waters. *Mar. Chem.,* 1:43–53.

Bishop, J.K.B., 1988. The barite-opal organic carbon association in oceanic particulate matter. *Nature,* 332:341–343.

Bowler, J. M., Hope, G. S., Jennings, J. N., Singh, G., and Walker, D., 1976. Late Quaternary climates of Australia and New Guinea. *Quat. Res.,* 6:359–399.

Broecker, W. S., and Peng, T.-H., 1982. *Tracers in the Sea:* Palisades, NY (Lamont Doherty Geological Observatory).

Broecker, W. S., Andree, M., Klaus, M., Bonani, G., Wolfli, W., Oeschger, H., 1988. New evidence from the South China Sea for an abrupt termination of the last glacial period. *Nature,* 333:156–158.

Calvert, S. E., 1990. Geochemistry and origin of the Holocene sapropel in the Black Sea. *In* Ittekot, V., Kempe, S., Michaelis, W., and Spitzy, A. (Eds.), *Facets of Modern Biogeochemistry,* Berlin (Springer-Verlag), 326–352.

Chappell, J., and Shackleton, N. J., 1986. Oxygen isotopes and sea level. *Nature,* 324:137–140.

Clemens, S. C., and Prell, W. L., 1990. Late Pleistocene variability of Arabian Sea summer monsoon winds and continental aridity: Eolian records from the lithogenic component of deep-sea sediments. *Paleoceanography,* 5:109–145.

COHMAP Members, 1988. Climatic changes of the last 18,000 years: observations and model simulations. *Science,* 241:1043–1052.

Curray, J. R., 1964. Transgressions and regressions. *In* Miller, R. C. (Ed.), *Papers on Marine Geology: Shephard Commemorative Volume:* New York (Macmillan), 175–203.

Exon, M. F., Haake, F.-W., Hartmann, M., Kolger, F.-C., Muller, P. J., and Whiticar, M. J., 1981. Morphology, water characteristics and sedimentation in the silled Sulu Sea, southeast Asia. *Mar. Geol.,* 39:165–195.

Fairbanks, R. G., 1989. A 17,000-year glacio-eustatic sea level record: influence of glacial melting rates on the Younger Dryas event and deep-ocean circulation. *Nature,* 342:637–642.

Fisher, K., Dymond, J., and Lyle, M., 1986. The benthic cycle of copper: evidence from sediment trap experiments in the eastern tropical North Pacific. *Geochim. Cosmochim. Acta,* 50:1535–1543.

Frische, A., and Quadfasel, D., 1990. Hydrography of the Sulu Sea. *In* Rangin, C., Silver, E. A., von Breymann, M. T., et al., *Proc. ODP, Init. Repts.,* 124: College Station, TX (Ocean Drilling Program), 101–104.

Gardner, J. V., Dean, W. E., and Wilson, C. R., 1984. Carbonate and organic-carbon cycles and the history of upwelling at DSDP Site 532, Walvis Ridge, South Atlantic Ocean. *In* Hay, W. W., Sibuet, J. C., et al., *Init. Repts. DSDP,* 75 (Pt. 2): Washington (U.S. Govt. Printing Office), 905–921.

Goldberg, E. D., and Arrhenius, G.O.S., 1958. Chemistry of Pacific pelagic sediments. *Geochim. Cosmochim. Acta,* 13:153–212.

Gordon, A. L., 1986. Interocean exchange of thermocline water. *J. Geophys. Res.,* 91:5037–5046.

Hovan, S. A., Rea, D. K., Pisias, N. G., and Shackleton, N. J., 1989. A direct link between the China loess and marine $\delta^{18}O$ records: aeolian flux to the North Pacific. *Nature,* 340:296–298.

Imbrie, J., Hays, J. D., Martinson, D. G., McIntyre, A., Mix, A. C., Morley, J. J., Pisias, N. G., Prell, W. L., and Shackleton, N. J., 1984. The orbital theory of Pleistocene climate: support from a revised chronology of the marine delta $\delta^{18}O$ record. *In* Berger, A., Imbrie, J., Hays, J., Kukla, G., and Saltzman, B. (Eds.), *Milankovitch and Climate* (Pt. 1): Dordrecht (D. Reidel), 269–305.

Jenkins, G. M., and Watts, D. G., 1968. *Spectral Analysis and Its Applications:* San Francisco (Holden Day).

Jumars, P. A., Altenbach, A. V., de Lange, G. J., Emerson, S. R., Hargrave, B. T., Muller, P. J., Prahl, F. G., Reimers, C. E., Steiger, T., and Suess, E., 1988. Transformation of seafloor arriving fluxes into the sedimentary record. *In* Berger, W. H., Smetaceck, V., and Wefer, G. (Eds.), *Productivity of the Ocean: Present and Past.* Dahlem Workshop Rep., Chichester (Wiley), 291–312.

Kukla, G., 1987. Loess stratigraphy in central China. *Quat. Sci. Rev.,* 6:191–219.

Kukla, G., and An, Z., 1989. Loess stratigraphy in central China. *Palaeogeogr., Palaeoclimatol., Palaeoecol.,* 72:203–225.

Kutzbach, J. E., 1981. Monsoon climate of the early Holocene: climate experiment with the earth's orbital parameters for 9000 years ago. *Science,* 214:59–61.

Kutzbach, J. E., and Guetter, P. J., 1986. The influence of changing orbital parameters and surface boundary conditions on climate simulations for the past 18,000 years. *J. Atmos. Sci.,* 43:1726–1759.

Kutzbach, J. E., and Otto-Bliesner, B. L., 1982. The sensitivity of the African-Asian monsoonal climate to orbital parameter changes for 9000 years B.P. in a low-resolution General Circulation Model. *J. Atmos. Sci.,* 39:1177–1188.

Labeyrie, L. D., Duplessy, J. C., and Blanc, P. L., 1987. Variations in mode of formation and temperature of oceanic deep waters over the past 125,000 years. *Nature,* 327:477–482.

Linsley, B. K., and Thunell, R. C., 1990. The record of deglaciation in the Sulu Sea: evidence for the Younger Dryas event in the western tropical Pacific. *Paleoceanography,* 5:1025–1039.

Linsley, B. K., Thunell, R. C., Morgan, C., and Williams, D. F., 1985. Oxygen minimum expansion in the Sulu Sea, western equatorial Pacific, during the last glacial low stand of sea level. *Mar. Micropaleontol.,* 9:395–418.

Lyle, M., and Collier, R., 1988. The oceanic copper cycle: a monitor of organic carbon flux. *Trans. Am. Geophys. Union,* 68:1772. (Abstract)

Lyle, M., Murray, D. W., Finney, B. P., Dymond, J., Robbins, J. M., and Brooksforce, K., 1988. The record of late Pleistocene biogenic sedimentation in the eastern tropical Pacific Ocean. *Paleoceanography,* 3:39–59.

Milliman, J. D., and Emery, K. O., 1968. Sea levels during the past 35,000 years. *Science,* 162:1121.

Milliman, J. D., and Meade, R. H., 1983. World wide delivery of river sediment to the oceans, *J. Geol.,* 91:1–21.

Morgan, C., 1983. The response of the Sulu Sea to late Quaternary climatic oscillations [thesis]. Univ. of South Carolina, Columbia.

Murray, S. P., and Arief, D., 1988. Throughflow into the Indian Ocean through the Lombok Strait, January 1985–January 1986. *Nature,* 333:444–447.

Oppo, D. W., and Fairbanks, R. G., 1989. Carbon isotope composition of tropical surface water during the past 22,000 years. *Paleoceanography,* 4:333–351.

Pisias, N., and Rea, D. K., 1988. Late Pleistocene paleoclimatology of the central equatorial Pacific: sea surface response to the southeast trade winds. *Paleoceanography,* 3:21–37.

Prell, W. L., 1984a. Monsoonal climate of the Arabian Sea during the late Quaternary: a response to changing solar radiation. *In* Berger, A. L., Imbrie, J., Hays, J., Kukla, G., and Saltzman, B. (Eds.). *Milankovitch and Climate* (Pt. 1): Dordrecht (D. Reidel), 349–366.

_____, 1984b. Variation of monsoonal upwelling: a response to changing solar radiation. *In* Hansen, J. E., and Takahashi, T. (Eds.), *Climatic Processes and Climate Sensitivity.* Am. Geophys. Union, Maurice Ewing Ser., 29:48–57.

Prell, W. L., and Curry, W. B., 1981. Faunal and isotopic indices of monsoonal upwelling: western Arabian Sea. *Oceanol. Acta,* 4:91–98.

Quadfasel, D., Kudrass, H., and Frische, A., 1990. Deep-water renewal by turbidity currents in the Sulu Sea. *Nature,* 348:320–322.

Quinn, W. H., 1974. Late Quaternary meteorological and oceanographic developments in the equatorial Pacific. *Nature,* 229:330–331.

Rangin, C., Silver, E. A., von Breymann, M. T., et al., 1990. *Proc. ODP, Init. Repts.,* 124: College Station, TX (Ocean Drilling Program).

Rottman, M. L., 1979. Dissolution of planktonic foraminifera and pteropods in the South China Sea sediments. *J. Foraminiferal Res.,* 9:41–49.

Schmitz, B., 1987. Barium, equatorial high productivity and the northward wandering of the Indian continent. *Paleoceanography.* 2:63–77.

Shackleton, N. J., 1977. Tropical rainforest history and the equatorial Pacific carbonate dissolution cycles. *In* Anderson, N. R., and Malahoff, A. (Eds.), *The Fate of Fossil Fuel CO_2* in the Oceans: New York (Plenum), 401–428.

Street, F. A., and Grove, A. T., 1979. Global maps of lake-level fluctuations since 30,000 yr B.P. *Quat. Res.,* 12:83–118.

Street-Perrott, F. A., and Harrison, S. P., 1985. Lake levels and climate reconstruction. *In* Hecht, A. D. (Ed.), *Paleoclimate Analysis and Modeling:* New York (Wiley), 291–340.

Street-Perrott, F. A., and Perrott, R. A., 1990. Abrupt climate fluctuations in the tropics: the influence of Atlantic Ocean Circulation, *Nature,* 343:607–612.

Thompson, P. R., Duplessy, J. C., and Bé, A. H., 1979. Disappearance of pink-pigmented *Globigerinoides ruber* at 120,000 yr BP in the Indian and Pacific Oceans. *Nature,* 280:554–558.

van Andel, T. H., Heath, G. R., and Moore, T. C., Jr., 1975. Cenozoic history and paleoceanography of the central equatorial Pacific. *Mem. Geol. Soc. Am.,* 143:1–134.

Van Riel, P. M., 1943. The Snellius Expedition 1929–1930, oceanographic results, Part V, *The Bottom Water,* Introductory Remarks and Oxygen Content, 2. Leiden (Brill), 1–76.

Webster, P. J., and Streten, N. A., 1978. Quaternary ice age climates of tropical Australia: interpretations and reconstructions. *Quat. Res.,* 10:10279–10309.

Wedepohl, K. H., 1970. Environmental influences on the chemical composition of shales and clays. *In* Ahrens, L. H., Press, F., Runcorn, S. K., Urey, H. C. (Eds.), *Physics and Chemistry of the Earth:* Oxford (Pergamon Press), 307–333.

Weliky, K., Suess, E., Ungerer, C. A., Muller, P. J., and Fisher, K., 1983. Problems with accurate carbon measurements in marine sediments and particulate matter in seawater: a new approach. *Limnol. Oceanogr.,* 28:1252–1259.

Wyrtki, K., 1961. *Scientific Results of Marine Investigations of the South China Sea and the Gulf of Thailand: Physical Oceanography of the Southeast Asian Waters:* Univ. of California, Scripps Inst. Oceanogr.

Date of initial receipt: 28 June 1990
Date of acceptance: 11 February 1991
Ms-124B-151

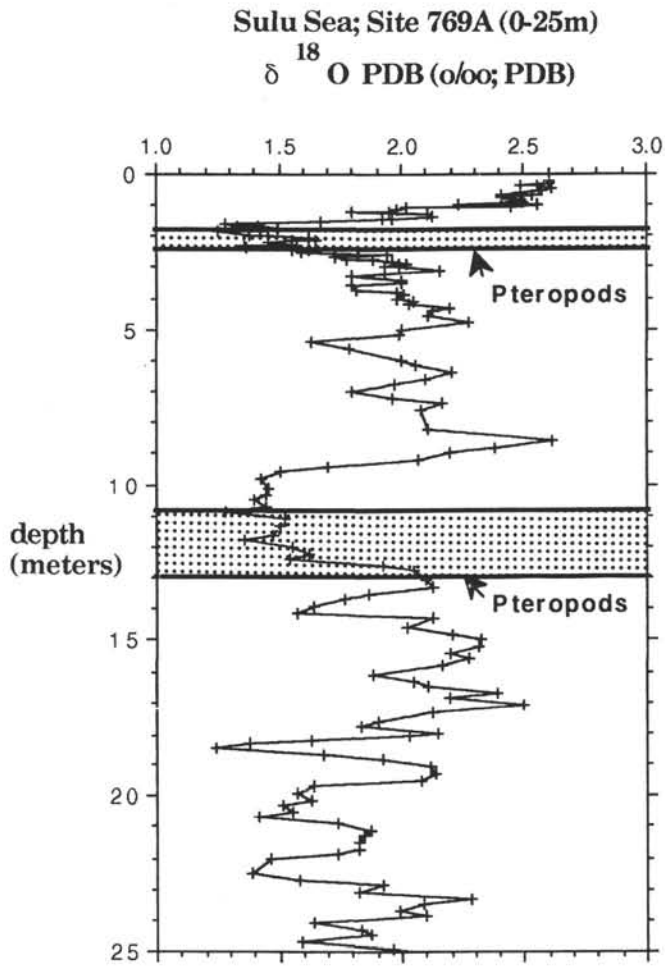

Figure 15. $\delta^{18}O$ and pteropods in the last 200 Ka of Hole 769A. Pteropods are found only in these two zones, in which they are abundant and well preserved.

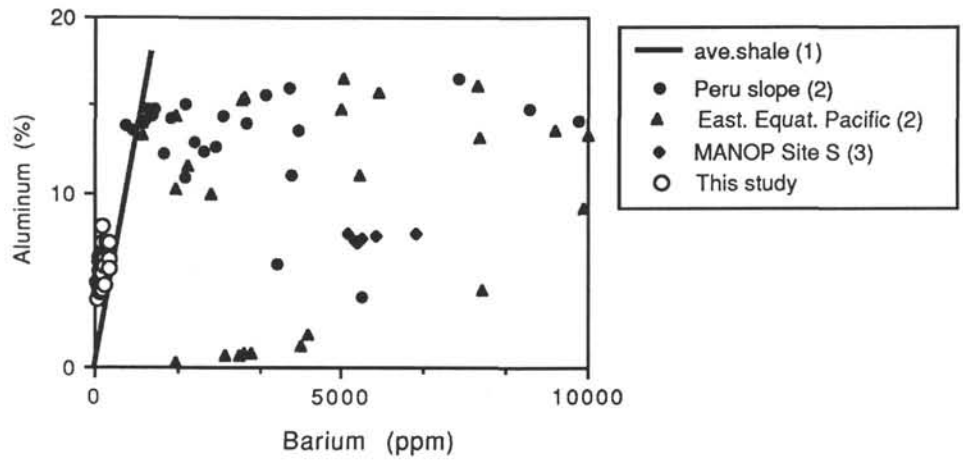

Figure 16. Barium concentration vs. aluminum for different environments. Open circles are samples from Hole 769A in the Sulu Sea, which cluster near the Ba/Al detrital ratio (solid line, Wedepohl, 1970). Data for the Peru Slope (closed circles) and eastern equatorial Pacific (closed triangles) are from von Breymann et al. (1990). MANOP Site S (closed diamonds) data are from Murray (1987). Note the barium enrichment in areas of high productivity.

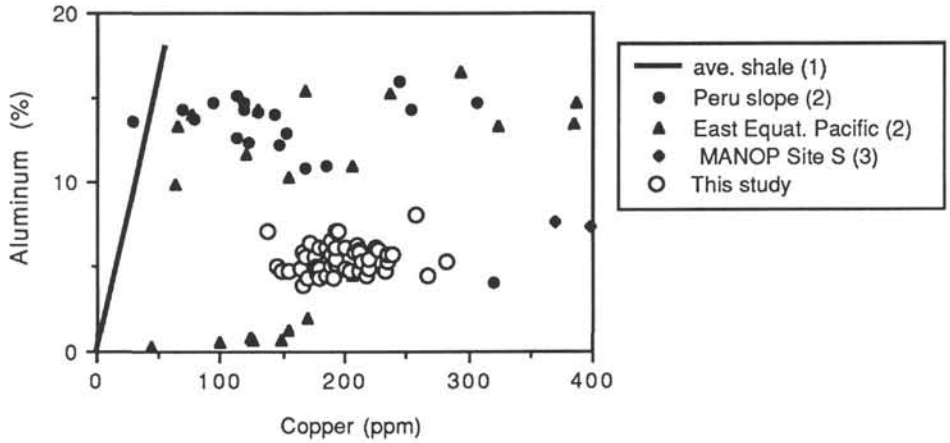

Figure 17. Copper concentration vs. aluminum for different environments. Open circles represent Sulu Sea Hole 769A. Note the copper enrichment relative to the detrital Cu/Al ratio (solid line, Wedepohl, 1970) similar to that observed in other high-productivity areas. Symbols and data sources are those given in Figure 16.

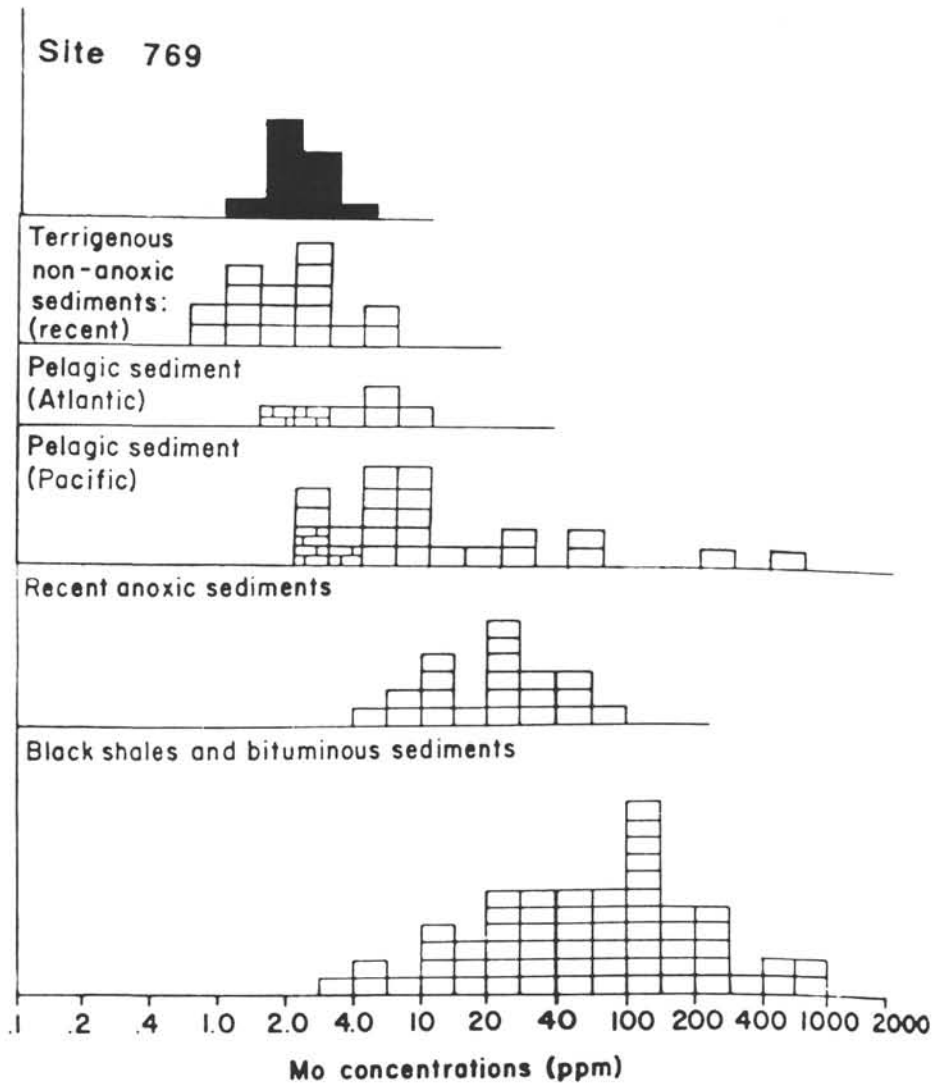

Figure 18. Molybdenum distribution in terrigenous, pelagic, anoxic and organic-rich sediments showing data from Site 769. Figure modified from Wedepohl, 1970.